JOURNAL OF MATERIALS SCIENCE 21 (1986) 4111–4116

# Phenomenological theory of Lüders bands

J. SCHLIPF
*Institut für Allgemeine Metallkunde und Metallphysik der Rheinisch Westfälischen Technischen Hochschule Aachen, FRG*

The constitutive functions of deformation, work hardening rate, $H$, and deceleration, $D$, are specialized for various deformation paths, and related to the evolution of dislocation structure. Based on the variation with deformation of $H$ and $D$ it is shown that two modes of tensile deformation may be defined: a destabilizing mode which leads to the normal homogeneous deformation behaviour terminated by necking and rupture, and a stabilizing mode which gives rise to Lüders band formation and subsequent homogeneous deformation. The conditions for Lüders banding are established and a simple mathematical description based on these concepts is given. A detailed discussion shows that with theories using only one structure parameter it is not possible to understand the Lüders phenomenon.

## 1. Introduction

Macroscopically non-uniform deformation processes in tension are observed in two forms: (i) necking and shear banding, where deformation is localized in space and changes with time; (ii) Lüders band propagation and jerky flow, where deformation bands with invariant deformation profiles move along the specimen. Both forms, however, grow from local instabilities. In order to treat these phenomena theoretically, the role of two independent factors has to be clarified: plastic instability and flow localization. Since the work of Considère [1] plastic instability in tension is known to occur if the hardening rate is not sufficient to outweigh geometrical softening. The instability point $\{\sigma_c; \varepsilon_c\}$ is given by the Considère criterion $d\sigma/d\varepsilon = \sigma$, where $\sigma$ and $\varepsilon$ denote local true stress and local true strain, respectively. On the other hand, flow localization involves spatial differences in strain or strain rate: localization occurs if gradients in strain or strain rate are accentuated [2]. While the Considère criterion is purely mechanical, localization criteria have to be derived from a consideration of the kinetics of deformation in space and time [3].

The deformation bands associated with Lüders deformation, after an initial nucleation period, usually exhibit quasistationary behaviour: an apparently invariant deformation profile moves at constant velocity, $v_L$, along the tensile axis. It has been shown elsewhere [4] that a truly stationary band at constant $v_L$ is possible only if the load, $P$, at constant nominal deformation rate, $v_M$, remains constant. Since Lüders strains are usually small, constant deformation rate is practically equivalent with constant extension rate, $v_M$. Historically the term Lüders band refers to the whole plastified region behind the band front. Plastic deformation, however, takes place mainly in a small region adjacent to the band front. In order to have a short term for this active plastic zone we call it L-band.

## 2. Constitutive functions

In this paper we report on the investigation of plastic deformation within the L-band, based upon the concept of evolution of the plastic state as developed by Hart [5], Mecking and Kocks [6], and others. Mecking and Kocks consider the dislocation contribution to the flow stress at constant temperature as a function $\sigma(\varrho, \dot{\varepsilon})$, where $\varrho$ (the overall dislocation density) characterizes the internal structure, and $\dot{\varepsilon}$ is the deformation rate. During deformation each individual volume element experiences a change in the flow stress which is determined by

$$d\sigma = \left.\frac{\partial\sigma}{\partial \ln \varrho}\right|_{\dot{\varepsilon}} d\ln\varrho + \left.\frac{\partial\sigma}{\partial \ln \dot{\varepsilon}}\right|_{\varrho} d\ln\dot{\varepsilon} \quad (1)$$

Thereby, the change of the flow stress is again decomposed into two contributions: the first term on the right-hand side of Equation 1 represents the internal stress fields of the forest dislocations and is related to the stored energy; the second term represents a generalized viscous stress and is related to the energy dissipated by moving dislocations in overcoming the barriers.

Upon integration, Equation 1 may be rewritten in the form

$$\Delta \ln \sigma = \Delta \ln \sigma_H + \Delta \ln \sigma_R \quad (2)$$

where $\Delta \ln \sigma$ is the total or dynamical hardening

$$\Delta \ln \sigma_H \equiv \int \frac{\partial \ln \sigma}{\partial \ln \varrho} d\ln\varrho = \text{strain hardening} \quad (3)$$

$$\Delta \ln \sigma_R \equiv \int \left.\frac{\partial \ln \sigma}{\partial \ln \dot{\varepsilon}}\right|_{\varrho} d\ln\dot{\varepsilon} = \text{viscous hardening} \quad (4)$$

In considering the change of $\sigma$ in a given volume element at $x$, time may be replaced by the local strain $\varepsilon$ [7]. This leads us to the evolution equation for the flow stress

$$\left.\frac{\partial \ln \sigma}{\partial \varepsilon}\right|_x = \left.\frac{\partial \ln \sigma}{\partial \ln \varrho}\right|_{\dot{\varepsilon}} \left.\frac{\partial \ln \varrho}{\partial \varepsilon}\right|_x + \left.\frac{\partial \ln \sigma}{\partial \ln \dot{\varepsilon}}\right|_{\varrho} \left.\frac{\partial \ln \dot{\varepsilon}}{\partial \varepsilon}\right|_x \quad (5)$$

0022–2461/86 $03.00 + .12 

Following the nomenclature of Kocks *et al.* [3] and Estrin and Mecking [7] we omit the subscript $x$ and define:

$$\left.\frac{\partial \ln \sigma}{\partial \ln \dot{\varepsilon}}\right|_{\varrho} \equiv M = \text{strain rate sensitivity} \tag{6}$$

$$\left.\frac{\partial \ln \sigma}{\partial \ln \varrho}\right|_{\dot{\varepsilon}} \frac{\partial \ln \varrho}{\partial \varepsilon} \equiv H = \text{work hardening rate} \tag{7}$$

While $M$ is a unique function of the state variables, $H$ is path dependent. For an unambiguous definition of $H$, therefore, the deformation path has still to be specified. For instance, if $\dot{\varepsilon}$ = constant,

$$H_{\dot{\varepsilon}} \equiv \left.\frac{\partial \ln \sigma}{\partial \ln \varrho}\right|_{\dot{\varepsilon}} \left.\frac{\partial \ln \varrho}{\partial \varepsilon}\right|_{\dot{\varepsilon}} \rightarrow \left.\frac{\partial \ln \sigma}{\partial \varepsilon}\right|_{\dot{\varepsilon}} = H_{\dot{\varepsilon}} \tag{8a, b}$$

By contrast, $(\partial \ln \sigma/\partial \varepsilon)_{\dot{\varepsilon}}$ alone is not a unique definition of $H$.

If the load $P$ is constant, we have

$$H_P \equiv \left.\frac{\partial \ln \sigma}{\partial \ln \varrho}\right|_{\dot{\varepsilon}} \left.\frac{\partial \ln \varrho}{\partial \varepsilon}\right|_{P} \rightarrow \left.\frac{\partial \ln \sigma}{\partial \varepsilon}\right|_{P} = 1 \tag{9a, b}$$

Finally, if $\sigma$ = constant,

$$H_\sigma \equiv \left.\frac{\partial \ln \sigma}{\partial \ln \varrho}\right|_{\dot{\varepsilon}} \left.\frac{\partial \ln \varrho}{\partial \varepsilon}\right|_{\sigma} \rightarrow \left.\frac{\partial \ln \sigma}{\partial \varepsilon}\right|_{\sigma} = 0 \tag{10a, b}$$

It is therefore desirable to distinguish between the work hardening rate, $H$, and the dynamical hardening rate

$$S \equiv \frac{\partial \ln \sigma}{\partial \varepsilon} \tag{11}$$

where $S$, like $H$, must be specified for the different deformation paths. Similarly, if $\dot{\varepsilon} = \dot{\varepsilon}(\sigma, \varrho)$, the evolution of the deformation rate may be considered:

$$\frac{\partial \ln \dot{\varepsilon}}{\partial \varepsilon} = \left.\frac{\partial \ln \dot{\varepsilon}}{\partial \ln \sigma}\right|_{\varrho} \frac{\partial \ln \sigma}{\partial \varepsilon} + \left.\frac{\partial \ln \dot{\varepsilon}}{\partial \ln \varrho}\right|_{\sigma} \frac{\partial \ln \varrho}{\partial \varepsilon} \equiv -D \tag{12}$$

which yields the relation

$$D = \frac{1}{M}(H - S) \tag{12a}$$

Again, by specifying the deformation path and comparing Equation 12 with Equations 8, 9 and 10, one finds:

$$D_\sigma \equiv -\left.\frac{\partial \ln \dot{\varepsilon}}{\partial \varepsilon}\right|_{\sigma} = \frac{H_\sigma}{M} \tag{13}$$

$$D_P \equiv -\left.\frac{\partial \ln \dot{\varepsilon}}{\partial \varepsilon}\right|_{P} = \frac{H_P - 1}{M} \tag{14}$$

Since $H_\sigma$ and $H_P$ may differ greatly, care must be exercised in relating $D$ and $H$ for the appropriate deformation path. In uniform deformation, as in creep tests, $D_\sigma$ and $D_P$ represent the deceleration of the deformation rate.

## 3. Stabilizing and destabilizing deformation modes

In the following we concentrate on plastic states at constant load $P$. While $D_P$ can be measured directly in an appropriate creep test, $H_P$ can be determined only theoretically from the evolution of the dislocation density or indirectly from Equation 14. For $M > 0$ deceleration is positive as long as $H_P > 1$. This means that fluctuations in $\dot{\varepsilon}$ would decrease with increasing $\varepsilon$ and therefore deceleration renders the deformation stable. Thus $D_P > 0$, by virtue of Equation 14 being equivalent to Considère's criterion in creep under constant load.

However, as deformation proceeds, $\varrho(\varepsilon)$ will eventually saturate. Consequently, $H_P$ will decrease until finally $H_P < 1$, and necking starts. Thus a transition from stable to unstable behaviour occurs at the stability limit $\varepsilon_D$, where $H_P = 1$. We may call such behaviour a destabilizing deformation mode. The reverse is true for the motion of an L-band. In this case deformation obviously starts with an accelerating rate ($D_P < 0$), as is signalled by the rapid load drop when the band is nucleated. Unlike the case of necking this unstable behaviour does not persist but turns into stable deformation characterized by decelerating $\dot{\varepsilon}$, until $\dot{\varepsilon} \approx 0$. This can be inferred from the fact that behind the L-band plastic deformation has ceased, or nearly so. We therefore conclude that a necessary prerequisite for Lüders band formation is the transition of $H_P < 1$ to $H_P > 1$ at the instability limit $\varepsilon_0$ where $H_P = 1$. Correspondingly we may call such behaviour a stabilizing deformation mode. The realization of the two modes is governed by the sign of the deceleration rate [4]:

$$\gamma_P \equiv \frac{\mathrm{d}D_P}{\mathrm{d}\varepsilon} = -\left.\frac{\partial^2 \ln \dot{\varepsilon}}{\partial \varepsilon^2}\right|_{P} \tag{15}$$

If $\gamma_P > 0$ (stabilizing mode) it is possible to have Lüders bands, if $\gamma_P < 0$ (destabilizing mode) one has uniform and continuous deformation.

It is interesting to compare the work hardening behaviour of the two modes at $P$ = constant, as can be inferred from the above considerations. Obviously, for both modes the dynamical hardening is given by

$$\Delta \ln \sigma = \varepsilon \tag{16}$$

This is represented by the straight lines in Fig. 1. Here the destabilizing mode (Fig. 1a) is characterized by the work hardening

$$\Delta \ln \sigma_H = \int_0^\varepsilon H_P \, \mathrm{d}\varepsilon > \Delta \ln \sigma \tag{17a}$$

and by the contribution of the viscous stress

$$\Delta \ln \sigma_R = -\int_0^\varepsilon M D_P \, \mathrm{d}\varepsilon < 0 \tag{17b}$$

On the contrary, the stabilizing mode (i.e. the Lüders band) obeys (Fig. 1b):

$$\Delta \ln \sigma_H = \int_0^\varepsilon H_P \, \mathrm{d}\varepsilon < \Delta \ln \sigma \tag{18a}$$

$$\Delta \ln \sigma_R = -\int_0^\varepsilon M D_P \, \mathrm{d}\varepsilon > 0 \tag{18b}$$

Thus $\dot{\varepsilon}$ must decrease or increase always in such a way

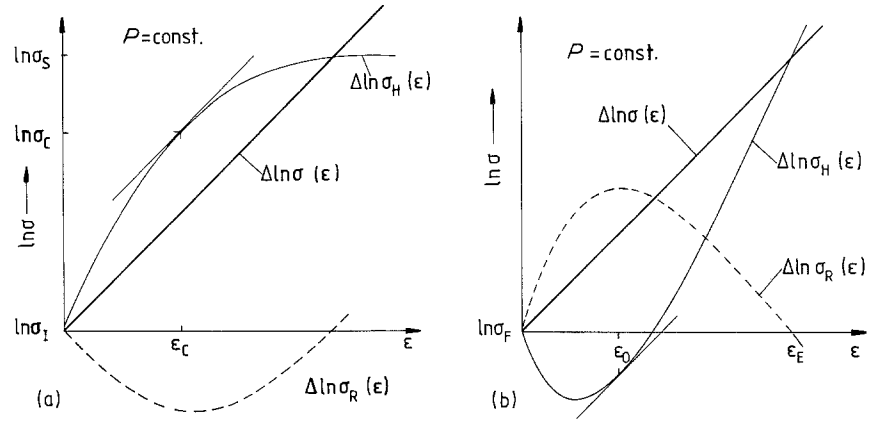


*Figure 1* Decomposition of the flow stress, $\sigma$, at constant load as a function of the true local strain. $\sigma_H$ = work hardening, $\sigma_R$ = viscous stress. (a) Destabilizing mode; $\sigma_c(\varepsilon_c)$ = ultimate tensile strength as given by Considère's construction; $\sigma_I$, $\sigma_S$ = initial and saturation stress, respectively. (b) Stabilizing mode, leading to L-band formation. $\sigma_F$ = stress at band front, $\varepsilon_0$ = centre of band, $\varepsilon_E$ = strain at effective band end.

that the viscous stress $\Delta \ln \sigma_R$ exactly balances the inequality Equations 17a or 18a, respectively.

If $M$ as defined by Equation 6 is set constant and inserted into Equation 4 we obtain

$$\Delta \ln \dot{\varepsilon} = \frac{1}{M} \Delta \ln \sigma_R = -\int_0^{\varepsilon} D_P \, d\varepsilon \quad (19)$$

This gives us, at least qualitatively, the dependence of $\Delta \ln \dot{\varepsilon}$ on $\varepsilon$ as shown in Fig. 2a for a Lüders band. When $\dot{\varepsilon}(\varepsilon)$ according to Equation 19 is known (Fig. 2b) we obtain $\varepsilon(t)$ (Fig. 3) as the inverse function of

$$t = \int_0^{\varepsilon} \frac{d\varepsilon}{\dot{\varepsilon}(\varepsilon)} \quad (20)$$

Finally, for stationary L-bands moving at constant speed $v_L$ we may set $\varepsilon(x, t) = y(z)$; $z = x - v_L t$. Then Equation 20 gives us

$$z(y) = \int_{\varepsilon_0}^{y} \frac{dy}{y'(y)} \quad (21)$$

where $y' \equiv dy/dz$, and $\varepsilon_0$ is the strain at the centre of the L-band (i.e. at $z = 0$).

## 4. A simple model for the L-band

$\Delta \ln \dot{\varepsilon}$ as depicted schematically in Fig. 2a appears to be well approximated by two pieces of parabola, or after differentiation by

$$-\left.\frac{\partial \ln \dot{\varepsilon}}{\partial \varepsilon}\right|_P = \begin{cases} 2\gamma_F(\varepsilon - \varepsilon_0); & 0 \leqslant \varepsilon \leqslant \varepsilon_0 \\ 2\gamma_E(\varepsilon - \varepsilon_0); & \varepsilon_0 \leqslant \varepsilon. \end{cases} \quad (22)$$

Writing $(\partial H/\partial \ln \sigma)_P \equiv (\partial H/\partial \varepsilon)_P \equiv C_P$ and setting $M$ = constant, comparison with Equation 15 gives us

$$\gamma_P(0) = 2\gamma_F = C_F/M;$$
$$\gamma_P(\varepsilon_E) = 2\gamma_E = C_E/M \quad (23)$$

$\varepsilon_E$ marks the strain at which $\dot{\varepsilon}$ has again fallen to $\dot{\varepsilon}_F$ (cf. Fig. 2b). It may be considered as a possible definition of band end.

In order to find solutions of Equation 22 which represent stationary L-bands, we make the transformations indicated above. Then the first integrals of Equation 22 are given by

$$\frac{1}{\varepsilon_0'}\frac{dy}{dz} = \begin{cases} \exp[-\gamma_F(y - \varepsilon_0)^2]; & 0 \leqslant y \leqslant \varepsilon_0 \quad (24a) \\ \exp[-\gamma_E(y - \varepsilon_0)^2]; & \varepsilon_0 \leqslant y \quad (24b) \end{cases}$$

The integration constant $-\varepsilon_0'$ is the maximum deformation gradient. It occurs at $y = \varepsilon_0$ which marks the centre of the L-band. These equations give the deformation gradient $y'$ as a function of the deformation $y$. It is depicted schematically in Fig. 2b. Since $\dot{\varepsilon} = -v_L y'$ it is clear that the deformation rate at the band front must jump from 0 to $\dot{\varepsilon}_F$. This discontinuity in $\dot{\varepsilon}$ is unavoidable as can be seen from the following argument. Assume there is no discontinuity. Then, in

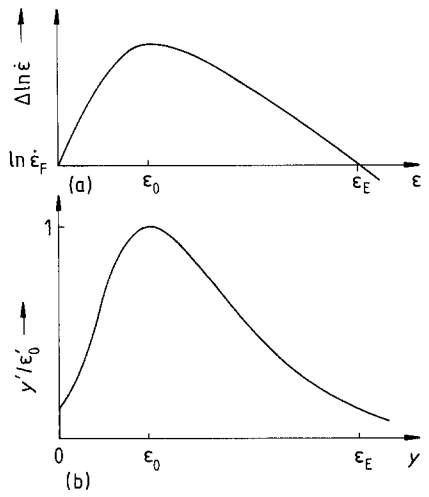


*Figure 2* (a) Schematic representation of the viscous stress according to Equation 19; (b) the corresponding deformation gradient in the L-band according to Equations 24a, b. The discontinuity at $y = 0$ is a consequence of the fact that the work hardening rate is finite.

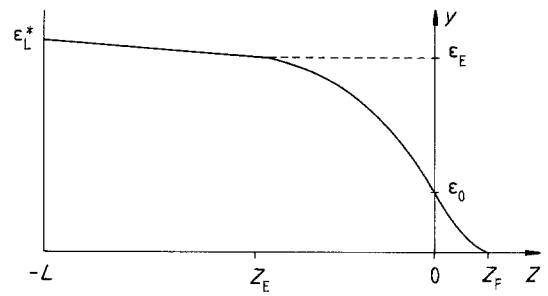


*Figure 3* Deformation profile of a moving Lüders band. $Z_F$ and $Z_E$ mark the positions of the band front and band end as defined by $y = 0$ and $y = \varepsilon_E$, respectively.

the vicinity of $\varepsilon \geqslant 0$ we may set $\dot{\varepsilon} = a\varepsilon^n$. This yields $\mathrm{d} \ln \dot{\varepsilon}/\mathrm{d}\varepsilon = n/\varepsilon$, which in the limit $\varepsilon \to 0$ according to Equation 14 would require $H_P \to -\infty$ or $M \to 0$. Both these limits are physically unfeasible.

A similar argument applies to the point marked $\varepsilon_E$ in Fig. 2. It would determine the true end of the L-band, if $\dot{\varepsilon}$ would become zero there: this would again require $H_P \to \infty$ or $M \to 0$ which has been rejected. Therefore, deformation cannot cease completely behind the L-band, there always remains some creep, however small. From Fig. 2b it is seen that $\varepsilon_E$ is the strain at which $\dot{\varepsilon}$ again takes the value $\dot{\varepsilon}_F$. Thus if $\dot{\varepsilon}_F \ll \dot{\varepsilon}_0$, the maximum strain rate, then $\varepsilon_E$ may well be taken as an effective Lüders strain. Otherwise, if creep behind the L-band is appreciable, the Lüders strain $\varepsilon_L$ as measured experimentally is a function of the length of the tensile specimen [4] and may differ appreciably from $\varepsilon_E$.

Introducing $y = 0$ and $y = \varepsilon_E$ into Equations 24a and 24b, respectively, we obtain

$$\dot{\varepsilon}_F = \dot{\varepsilon}_0 \exp(-\gamma_F \varepsilon_0^2) \tag{25a}$$

$$\varepsilon_E = \varepsilon_0[1 + (\gamma_F/\gamma_E)^{1/2}] \tag{25b}$$

Although all parameters characterizing the L-band can be obtained from the $y'(y)$-diagram, it would be desirable to have an analytical expression for the deformation profile. This requires an integration of Equation 24 which can be accomplished in terms of the function

$$\phi(y) \equiv \int_0^y \exp(x^2)\,\mathrm{d}x \tag{26}$$

The result, depicted schematically in Fig. 3, is given by

$$y - \varepsilon_0 = \begin{cases} \dfrac{1}{\gamma_F^{1/2}} \phi^{-1}(\gamma_F^{1/2}\varepsilon_0' z); & 0 \leqslant z \leqslant z_F \\ \dfrac{1}{\gamma_E^{1/2}} \phi^{-1}(\gamma_E^{1/2}\varepsilon_0' z); & z \leqslant 0 \end{cases} \tag{27}$$

where $\phi^{-1}(x)$ represents the inverse function of Equation 26, and $z_F$ gives the position of the band front. An effective width of the L-band may be defined by $W_L = \varepsilon_L/\varepsilon_0'$.

Although during nucleation of the L-band the deformation path is not specified, we may use Equation 22 for a quantitative demonstration of the localization condition. It is highly probable that nucleation takes place at a soft spot or at stress concentrations where the yield stress has a local minimum. Also the behaviour of the deformation apparatus as described by the machine equation

$$\dot{\sigma}_a = \frac{E_M}{L}\left[v_M - \int_0^L \dot{\varepsilon}\,\mathrm{d}x\right] \tag{28}$$

is important. Here, $\sigma_a = P/A_0$ is the applied stress, $E_M$ = effective modulus of the stretching system, $v_M$ = cross head speed, $L$ = length of specimen. Single L-bands will form only if during nucleation the local deformation rate is so high that the maximum stress $\sigma_M$ reached is smaller than the average yield stress $\langle\sigma_{ya}\rangle$ of the specimen. Otherwise homogeneous deformation would occur. The chance for $\sigma_M < \langle\sigma_{ya}\rangle$ will be the greater, the smaller $\varepsilon_M$ is, where $\varepsilon_M$ is the strain at which $\sigma = \sigma_M$ (cf. Fig. 4). The maximum stress $\sigma_M$ will be reached when $\dot{\sigma}_a = 0$, i.e. when $\int \dot{\varepsilon}\,\mathrm{d}x = v_M$. In the range $\varepsilon < \varepsilon_0$ Equation 24a yields

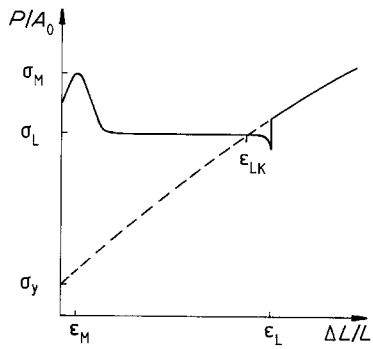


*Figure 4* Load–elongation diagram for steady state Lüders band. Local strains $\varepsilon_M$, $\varepsilon_{LK}$, $\varepsilon_L$ are explained in the text. Nominal stresses $\sigma_M$ and $\sigma_L$ represent nucleation stress and propagation stress, respectively. $\sigma_y$ denotes the yield stress for homogeneous deformation.

$$\dot{\varepsilon} = \dot{\varepsilon}_0 \exp[-\gamma_F(\varepsilon - \varepsilon_0)^2] \tag{29}$$

Assuming a uniform deformation rate in a narrow region of width $w$ as a crude approximation for the nucleation event and with $v_M$ satisfying $w\dot{\varepsilon}_F < v_M < w\dot{\varepsilon}_0$ we have

$$\int_0^w \dot{\varepsilon}\,\mathrm{d}x \approx w\dot{\varepsilon}_0 \exp[-\gamma_F(\varepsilon - \varepsilon_0)^2] = v_M \tag{30}$$

When Equation 25a is inserted into Equation 30 one obtains after solving for $\varepsilon_M$:

$$\varepsilon_M = \frac{1}{\gamma_F^{1/2}}\left[\left(\ln\frac{\dot{\varepsilon}_0}{\dot{\varepsilon}_F}\right)^{1/2} - \left(\ln\frac{w\dot{\varepsilon}_0}{v_M}\right)^{1/2}\right] \tag{31}$$

Since the logarithmic terms can produce only small variations, the order of magnitude of $\varepsilon_M$ is given by $1/\gamma_F^{1/2} \sim [M/C_P(0)]^{1/2}$. Thus, as in necking, a small strain rate sensitivity favours localization. It should be noted, however, that for Lüders band formation the initial slope of the work hardening rate, $C_P(0)$, is equally important.

It is apparent from Equation 27 that in a phenomenological description the shape of the L-band is determined by the two integration constants $\varepsilon_0$ and $\varepsilon_0'$ which cannot be reduced to phenomenological material parameters. They are related to the microscopic processes in the band.

## 5. The Lüders strain

Usually the actual deformation is concentrated in a L-band of width $W_L \ll L_0$, the initial length of the tensile bar. However, the Lüders strain, $\varepsilon_L$, as measured experimentally (cf. Fig. 4) still contains contributions from creep deformation in the wake of the L-band and from the non-stationary processes during nucleation and termination of the band. Therefore, in order to obtain a theoretical estimate of $\varepsilon_L$ we make the following simplifying assumptions: (i) we consider an infinite tensile bar with the gauge length $L_0$ indicated by markers at $x = -L_0$; $x = 0$; (ii) upon stretching, a fully developed L-band moves from $-\infty$ to $+\infty$. At $t = 0$ the band centre ($\varepsilon = \varepsilon_0$) is at $x = -L_0$. While the band moves the gauge length

changes from $L_0$ to $L$ so that the propagation time of the band is given by $t_p = L/v_L$ and the marker at the initial position $x = -L_0$ is shifted to $x = -L$; the effective width of the L-band, $W_L \ll L_0$. Then $\varepsilon_L^*$, the strain at $x = -L$ reached after $t_p$, is very close to the experimental value $\varepsilon_L$. According to Equation 20

$$t_p = \frac{L}{v_L} = \int_0^{\varepsilon_L^*} \frac{d\varepsilon}{\dot{\varepsilon}(\varepsilon)} \tag{32}$$

Introducing $\varepsilon_L^*$ instead of $\varepsilon_L$ into the well-known relations $v_L = v_M/\varepsilon_L$ and $L = L_0 \exp(\varepsilon_L)$, we obtain

$$\varepsilon_L^* = \frac{v_M}{L_0} \exp(-\varepsilon_L^*) \int_0^{\varepsilon_L^*} \frac{d\varepsilon}{\dot{\varepsilon}(\varepsilon)} \tag{33}$$

As is easily seen, this is equivalent to using the inverse function of Equation 21 and setting $z = -L$. In the model presented above Equation 21 yields

$$\varepsilon_L^* = \varepsilon_0 + \frac{1}{\gamma_E^{1/2}} \phi^{-1}(-\varepsilon_0' L_0 \gamma_E^{1/2} e^{\varepsilon_L^*}) \tag{34}$$

$$z_F = \frac{1}{-\varepsilon_0' \gamma_F^{1/2}} \phi(\varepsilon_0 \gamma_F^{1/2}) \tag{35}$$

## 6. Discussion

In the preceding sections it was shown that three requirements must be met in order to obtain an L-band:

(i) initial instability: $D_P(0) < 0$
(ii) stabilizing mode: $\gamma_P > 0$
(iii) localization condition: $\gamma_P(0) \gg 1$.

The first of these conditions is equivalent to $H_P < 1$; $M > 0$ or $H_P > 1$; $M < 0$ for $\varepsilon < \varepsilon_0$. While it is generally accepted that $M < 0$ is a condition for serrated flow, the L-bands considered here form in material states where $M > 0$. Thus our condition for L-band formation is $H_P < 1$; $\varepsilon < \varepsilon_0$. This is at variance with the proposition of Wijler *et al.* [8] who give $H_{\dot{\varepsilon}} < 0$. The latter condition is probably inferred from the fact that the initial slope of the load–elongation curve is negative when a Lüders band is formed. However, this reflects only the nucleation event, while during spreading of the band the load remains constant.

It is easily seen that the above conditions cannot be satisfied in theories employing only one structure parameter. These theories can describe only continuous deformation. According to Mecking and Kocks [6] the plastic behaviour in continuous tensile deformation of most metallic materials may be rationalized in the form

$$\sigma(\varrho, \dot{\varepsilon}) = \alpha_0 G \boldsymbol{b} [\varrho(\varepsilon)]^{1/2} (\dot{\varepsilon}/\hat{\dot{\varepsilon}})^M \tag{36}$$

where $\hat{\dot{\varepsilon}}$ = constant refers to a reference state, $G$ is the shear modulus, $\boldsymbol{b}$ is the Burgers vector, and $\alpha_0 \approx 0.5$. as shown by Estrin and Mecking [7], this one-parameter-approach yields in the case of constant load:

$$\left(\frac{\dot{\varepsilon}}{\dot{\varepsilon}_s}\right)^n = A_1 + A_2 \varepsilon + A_3 \exp(-\varepsilon/\varepsilon_r) \tag{37}$$

where $A_1$, $A_2$, $A_3$, $\varepsilon_r$, $\varepsilon_s$, and $n$ are constants $> 0$. Inspection of this equation reveals that indeed it represents a destabilizing mode only ($\gamma_P < 0$ throughout).

Stabilizing modes can be obtained, if the mobile dislocation density $\varrho_m(\varepsilon)$ is introduced as an additional structure parameter. The mobile dislocation density has been considered in previous theories of the Lüders phenomenon [9–11]. In these theories, however, no clear distinction is made between mobile and immobile dislocations. A linear superposition

$$\sigma = \hat{\sigma}(\varepsilon) + \sigma_1(\dot{\varepsilon}/\hat{\dot{\varepsilon}})^M \tag{38}$$

for the dislocation components of the flow stress is used which is at variance with Equation 36. Moreover, the evolution of the forest dislocation structure is neglected. These are serious deficiencies, since the superposition is essentially non-linear as revealed by the constitutive laws Equations 2 or 29, and the evolution of the forest density, $\varrho$, is important for the development of the work hardening rate, $H_P$. A detailed model including these features will be given in a forthcoming paper [12].

As noted by Gilman [10], creep curves $\dot{\varepsilon}(\varepsilon)$ of LiF resemble the $\varepsilon$-curves in Lüders banding (cf. Fig. 2b). This kind of creep, however, is qualitatively different from creep as described by Equation 37. It is also observed in creep of germanium and silicon [14]. If these materials are deformed in tension, they show an upper and lower yield point, but no Lüders band, i.e. an initial stabilizing mode without localization. These yield point phenomena are usually attributed to an initial scarcity of mobile dislocations. It is therefore concluded that the evolution of the mobile dislocation density plays a dominant role in the development of a stabilizing mode.

In his work on non-uniform deformation, Kocks [13] sets $\varepsilon_0 = 0$; $\dot{\varepsilon}_F = \dot{\varepsilon}_0$ which is tantamount to letting $\gamma_F \to \infty$. This implies $C_F \to \infty$ or $M \to 0$ which is quite unrealistic. Kocks also proposes for the propagation stress $\Delta\sigma_L \equiv \sigma_L - \sigma_y$ (cf. Fig. 4):

$$\Delta\sigma_L = \theta \varepsilon_{LK} \tag{39}$$

$$\Delta\sigma_L = \sigma_L M \ln(\dot{\varepsilon}_F/\langle\dot{\varepsilon}\rangle) \tag{40}$$

Here $\langle\dot{\varepsilon}\rangle = (1/L) \int_0^L \dot{\varepsilon}\, dx$ is the average deformation rate, $\theta$ is the linear work hardening rate at $\dot{\varepsilon} = \langle\dot{\varepsilon}\rangle$, and $\varepsilon_{LK}$ is the Lüders strain as defined operationally by Kocks (cf. Fig. 4).

Writing $\dot{\varepsilon} = \varrho_m \boldsymbol{b} v_D$, where $v_D$ is the average velocity of dislocations, the increase of $\dot{\varepsilon}$ from zero to a peak value as postulated by Kocks will appear as a jump if the acceleration time can be neglected. This is possible only if the density of mobile dislocations is very high. However, in the undeformed region, and therefore also at the band front, $\varrho_m$ must be small, otherwise a Lüders band would not form. The time needed for dislocation multiplication will certainly be much longer than the acceleration time. Thus $\dot{\varepsilon}_F$ must be small and Equation 40 cannot be correct. In the present model the increase of $\dot{\varepsilon}$ occurs with a finite slope and the extra stress at the band front is attributed to the lack of mobile dislocations.

## References


1. A. CONSIDÈRE, *Ann. des Ponts Chaussèes* **9** (1885) 574.
2. E. W. HART, *Acta Metall.* **15** (1967) 351.
3. U. F. KOCKS, J. J. JONAS and H. MECKING, *ibid.* **27** (1979) 419.
4. J. SCHLIPF, *Z. Metallkde* **75** (1984) 517.
5. E. W. HART, *Acta Metall.* **18** (1970) 599.
6. H. MECKING and U. F. KOCKS, *ibid.* **29** (1981) 1965.
7. Y. ESTRIN and H. MECKING, *ibid.* **32** (1984) 57.
8. A. WIJLER and J. SCHADE VAN WESTRUM, *Scripta Metall.* **5** (1971) 531.
9. G. T. HAHN, *Acta Metall.* **10** (1962) 727.
10. J. J. GILMAN, *J. Appl. Phys.* **36** (1965) 2772.
11. K. REIFF and K. LÜCKE, *Arch. Eisenhüttenw.* **50** (1979) 527.
12. J. SCHLIPF, *Mater. Sci. Eng.* **77** (1986) 19.
13. U. F. KOCKS, Kinetics of Nonuniform Deformation, in "Progress in Materials Science, Chalmers Anniversary Volume", (Pergamon, Oxford, 1981) p. 185.
14. B. REPPICH, P. HAASEN and B. ILSCHNER, *Acta Metall.* **12** (1964) 1283.



*Received 16 December 1985*
*and accepted 24 April 1986*